ACADEMIC PRESS

Biochemical and Biophysical Research Communications 293 (2002) 489–496

BBRC

www.academicpress.com

Crystal structure of the liganded anti-gibberellin A_4 antibody 4-B8(8)/E9 Fab fragment☆

Takashi Murata,[a,*] Shinya Fushinobu,[b] Masatoshi Nakajima,[a] Osamu Asami,[c] Takeshi Sassa,[d] Takayoshi Wakagi,[b] and Isomaro Yamaguchi[a]

[a] *Department of Applied Biological Chemistry, Division of Agriculture and Agricultural Life Sciences, The University of Tokyo, 1-1-1 Yayoi, Bunkyo-ku, Tokyo 113-8657, Japan*

[b] *Department of Biotechnology, Division of Agriculture and Agricultural Life Sciences, The University of Tokyo, 1-1-1 Yayoi, Bunkyo-ku, Tokyo 113-8657, Japan*

[c] *Biotechnology Division, Toyota Central R&D Labs., Inc., 41-1 Aza Yokomichi, Oaza Nagakute, Nagakute-cho, Aichi-gun, Aichi 480-1100, Japan*

[d] *Department of Bioresource Engineering, Faculty of Agriculture, Yamagata University, 1-23 Wakaba-cho, Tsuruoka-shi, Yamagata 997-8555, Japan*

Received 11 March 2002

Abstract

Gibberellins, a class of plant hormones, consist of more than 120 members. Only a few of them are recognized by a receptor that remains unknown. The haptenic mouse monoclonal antibody, 4-B8(8)/E9, was generated against gibberellin A_4 (GA_4) to recognize biologically active GA selectivity, and we attempted to confirm the binding properties between the antibody and GA_4. We carried out an X-ray crystallographic analysis of the 4-B8(8)/E9 Fab fragment complexed with GA_4 at a 2.8 Å resolution by using the molecular replacement method. The crystal structure of the Fab fragment showed the typical immunoglobulin fold of the β-barrel structure which is the common motif of all antibodies. A small hapten-combining site was made up of three heavy chain CDR loops. On the other hand, CDRs of the light chain did not interact directly with GA_4. The C/D rings of the GA_4 molecule were in van der Waals contact mainly with the aromatic side chain of Tyr100AH and Phe100BH of CDR-H3. The 3β-hydroxyl and 6β-carboxyl groups were, respectively, hydrogen-bonded to the main chain of Ala33H and to the Thr53H heavy chain.

Keywords: Gibberellin; Antibody; Plantibody; Crystal structure

Gibberellins (GAs, Fig. 1) are a class of plant hormones and play important roles in various plant growth phenomena, including seed germination, stem elongation, and flower development [1]. They form a large family of diterpenoids, which has over 120 homologs. In such a large family, only some GAs with certain structural features are biologically active by themselves. They carry 3β-hydroxyl, 6β-carboxyl, and 4α–10α γ-lactone groups as GA_1, GA_3, GA_4, GA_7, and several others, and are called "bioactive GAs". Studies on the structure–activity relationship show that a receptor, which remains unidentified, recognizes limited numbers of GAs, and interest has increased in the manner by which a receptor protein can recognize [2]. We have previously prepared and applied the anti-GA antibodies to analyze GAs and plant growth regulation [3–5]. The mouse monoclonal antibody designated 4-B8(8)/E9 was raised against GA_4 and showed high binding selectivity against active GAs. On the other hand, the antibody did not recognize biologically inactive GAs, with very few exceptions. This antibody can therefore critically recognize the 3β-hydroxyl and 6β-carboxyl groups of GA molecules which are considered to be es-

☆ *Abbreviations:* GA, gibberellin; GA_n, gibberellin A_n; CDR, complementarity-determining region; scFv, single-chain variable fragment; Fab, antigen-binding fragment of the antibody; Fc, crystallizable fragment of the antibody; V_L, variable region of the light chain; C_L, constant region of the light chain; V_H, variable region of the heavy chain; C_{Hn}, constant region of the heavy chain *n*; IgG, immunoglobulin G; NCS, non-crystallographic symmetry; PBS, phosphate buffered saline; SDS–PAGE, sodium dodecyl sulfate–polyacrylamide gel electrophoresis; Tris, tris-(hydroxymethyl)-aminomethane; Bis-Tris, bis-(2-hydroxyethyl)-iminotris-(hydroxymethyl)-methane

* Corresponding author: Fax: +81-3-5841-8025.
E-mail address: tks@pgr1.ch.a.u-tokyo.ac.jp (T. Murata).

0006-291X/02/$ - see front matter
PII: S0006-291X(02)00225-5

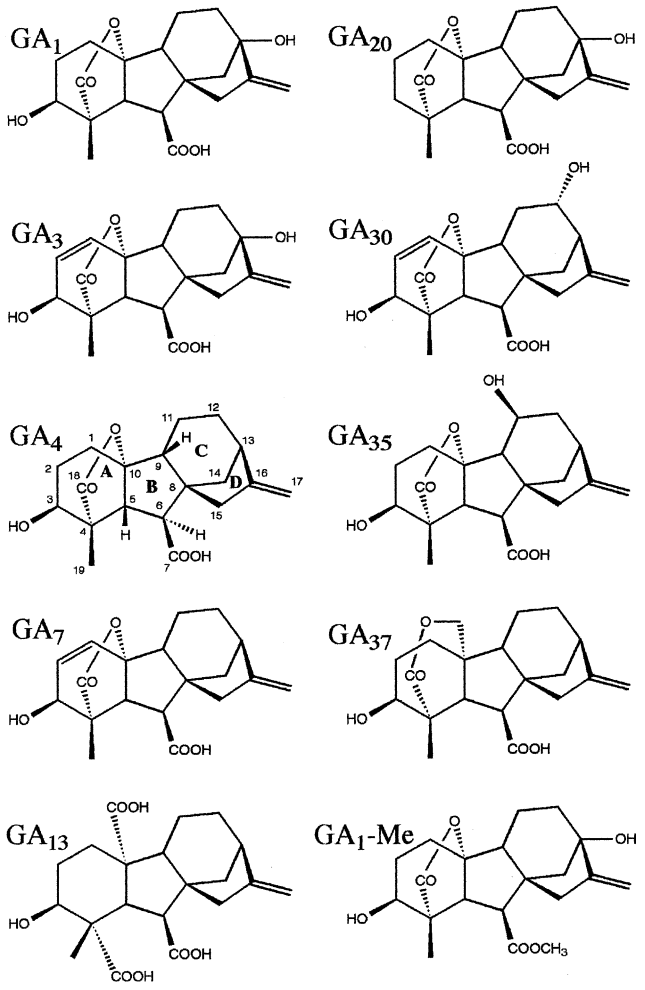

GA_1	128	GA_{20}	< 0.01
GA_3	17	GA_{30}	26
GA_4	100	GA_{35}	3
GA_7	64	GA_{37}	150
GA_{13}	10	GA_1-Me	< 0.01

Fig. 1. Structures of GAs. GA_1, GA_3, GA_4, and GA_7 are biologically active GAs. The atom numbering and ring name are labeled for GA_4. The cross-reactivity of the 4-B8(8)/E9 antibody against GAs are shown in the lower box [2].

sential for showing biological activities in plants. The three-dimensional structure of the antigen-combining site of this antibody can thus be expected to mimic the ligand binding site of the GA receptor [2].

Antibodies or their fragments produced in a plant are often called plantibodies and have been used for immunomodulating the plant metabolism and/or pathogen resistance. Conrad and Fiedler [6] have succeeded in expressing a single-chain variable fragment (scFv) of an anti-abscisic acid antibody and in modulating the effect of abscisic acid which is one of the plant hormones. We have also succeeded in expressing the anti-GA_{24} antibody in tobacco and in reducing the plant height by trapping GA_{24}, a biosynthetic intermediate of GA_4. We have tried to construct an scFv of the anti-GA_4 antibody, 4-B8(8)/E9, but failed to express this scFv in an active form. A crystallographic analysis of a conjugate of the antibody with GA_4 would help to both project hapten–antibody interaction and to design an improved scFv for acquiring binding activity.

Several enzymes participating in the biosynthesis and catabolism of GAs were purified, and their cDNAs were cloned. Some of their recombinant proteins were proved to show enzyme activity, however, none of them were determined in respect of their three-dimensional structure. A crystallographic analysis of the antibody-GA_4 conjugate would provide imformation about the three-dimensional structure that can recognize the functional group essential to biological activity.

Antibody molecules are composed of light and heavy polypeptide chains, each having variable and constant regions. Digestion of the whole antibody molecule, using such proteases as papain and ficine, gives Fab and Fc fragments. Antigen recognition is carried by the Fab fragment, which consists of the light chain (V_L and C_L) and the amino-terminal half of the heavy chain (V_H and C_{H1}). Each portion of the amino-terminals of light and heavy chains contains three regions of highly variable length and sequence, the complementarity-determining regions (CDRs), which determine the conformation of the antigen-combining site and confer specific binding activity to the antibody molecule. The antigen-combining site is constructed on an immunoglobulin fold that is essentially common to all antibody molecules and forms the scaffold supporting the hypervariable loops.

Many three-dimensional structures of the complex between an antibody and antigen protein or peptide had been resolved by X-ray crystallography [7–20]. These studies have permitted a detailed description of the antigenic determinants and of the antibody combining site. They also have provided critical information on the characteristics of protein–protein and protein–peptide complexes. In contrast, there have been few studies of the crystal structure between an antibody and haptenic antigen such as that occurring in natural products, and information about ligand recognition against small organic compounds is little known.

We report here the three-dimensional structure of the GA_4 liganded Fab fragment of the 4-B8(8)/E9 antibody determined by X-ray crystallography at 2.8 Å resolution. This structural investigation of the 4-B8(8)/E9 Fab fragment elucidates the antigen-combining area, key amino acid residues, and local conformation of the hypervariable loops for the recognition of GA_4.

Materials and methods

Preparation of the 4-B8(8)/E9 Fab fragment. Production of the hybridoma clones and preparation of the ascites fluid have been pre-

viously reported [2]. The monoclonal antibody, 4-B8(8)/E9, was precipitated by treating the ascites fluid with 50% saturated ammonium sulfate dissolved in a 1:1 mixture of phosphate-buffered saline (PBS) and the ImmunoPure IgG Binding buffer (Pierce), and then purifying in an immobilized protein A column (2.5 ml in volume, Pierce) with the ImmunoPure IgG Binding buffer and the ImmunoPure IgG1 Mild Elution buffer (6 ml, Pierce). SDS–PAGE showed that the IgG sample was pure enough for further experiments after the affinity purification.

The antibody was cleaved into its Fab and Fc fragments with an ImmunoPure Fab Preparation kit (Pierce). The Fab fragment was recovered from the reaction mixture by passing through a protein A column, which effectively retained the Fc fragment and undigested IgG, and purifying by gel filtration column chromatography (Sephacryl HR-50, 10 mm $\varnothing \times 250$ mm), eluting with a 50 mM Tris–HCl buffer at pH 7.0. SDS–PAGE of the purified Fab fragment showed two bands at 25 kDa.

Crystallization. Crystals of the GA_4 liganded Fab fragment of 4-B8(8)/E9 were obtained at 30 °C by the sitting drop vapor diffusion method from a reservoir solution comprising 20%(v/v) glycerol, 12%(w/v) polyethylene glycol 3350, and 0.06 M Bis-Tris–HCl at pH 6.5. The protein drops contained 3 μl of 8 mg/ml of the liganded Fab fragment solution and 3 μl of the reservoir solution. Crystals of dimensions $0.15 \times 0.15 \times 0.05$ mm grew within one week.

Crystallography. X-ray diffraction data were collected for a single well-shaped crystal at 100 K by using the BL18B unit of the Photon Factory at the High Energy Accelerator Research Organization (KEK), Japan. Auto-indexing and data processing were performed with the DPS/Mosflm [21] program and are summarized in Table 1.

Table 1
Data collection, processing, and refinement statistics

(a) *Data collection and processing*	
Wavelength (Å)	1.0
Temperature (K)	100
Resolution limits (Å)	2.7
Total no. of observed reflections	402,565
Completeness (%)	100
of last shell (2.85–2.70 Å)	100
No. of unique reflections	26,460
R_{merge}[a] (%)	8.2
of last shell (2.85–2.70 Å)	3.21
Space group	$C222_1$
Unit cell (Å)	$a = 1181$, $b = 150.1$, $c = 106.9$ $\alpha = \beta = \gamma = 90°$
(b) *Refinement*	
Resolution limits (Å)	2.8
No. of reflections in refinement	22,549
Final model	
No. of heterodimers in an asymmetric unit	2
No. of protein atoms	6671
No. of residues	882
No. of water molecules	130
R-factor[b] (%)	23.4
R_{free}[c] (%)	29.6
R.m.s deviations from ideal values	
Bond lengths (Å)	0.007
Bond angles (°)	1.4

[a] $R_{merge} = \sum \sum_i |I(h)_i - \langle I(h) \rangle| / \sum \sum_i |I(h)_i|$, where $\langle I(h) \rangle$ is the mean intensity of equivalent reflections.

[b] $R = \sum |F_o - F_c| / \sum |F_o|$, where F_o and F_c are the observed and calculated structure factor amplitudes, respectively.

[c] $R_{free} = \sum |F_o - F_c| / \sum |F_o|$, calculated using a test data set, 5% of total data randomly selected from the observed reflections.

A preliminary model of the crystal structure of the Fab fragment was obtained by the molecular replacement method with the CNS program [22]. A murine Fab fragment (PDB entry 1IKF [23]) was used as the search model. A cross-rotation function search of the data was performed between a 15 and 4 Å resolution. The highest peak in the rotation function list was about twice that of the next peak. A translation search of the data was also performed between a 15 and 4 Å resolutions. There were two Fab fragments in the asymmetric unit, these being related by a pseudo twofold axis of non-crystallographic symmetry (NCS).

To construct a suitable starting model for crystallographic refinement, a mouse disulfide-stabilized Fv antibody (PDB entry 1DSF [24]) was replaced with the variable region of 1IKF, because of its high similarity in sequences (89.3% identity for V_L and 72.9% for V_H). This substituted model was duplicated and placed at the position of the molecular replacement solution. The chains of one of the two Fab fragments in the asymmetric unit are named the L and H chains, and those of the other Fab fragment are named the M and I chains.

Three steps of rigid body refinement were applied with the data to a 2.8 Å resolution. First, the two Fab fragments were treated as independent rigid bodies, before individual refinement of the light and heavy chains of each fragment. Next, the variable and constant domains of both fragments were allowed to adjust to their positions. This procedure reduced the crystallographic R-value to 0.404.

A subsequent simulated-annealing refinement (5000 K) and group B-factor refinement reduced the R-value 0.291. NCS restraint between the two Fab fragments in the asymmetric unit was applied with a weight of 150 kcal mol^{-1} Å^{-2} on the following regions: L1–L45, L47–L60, L65–L109, H4–H44, H46–H97, and H110–H121.

The initial $2F_o$–F_c electron density map and density modification map showed reasonable traces within the β-barrel structure of the immunoglobulin fold and CDR loops, except for CDR-H3. Program O [25] was used to substitute amino acids different from those in the initial molecule and for electron density map fitting. The energy-minimized hapten structural model was constructed with CS ChemOffice software (CambridgeSoft). The model of GA_4 was built into the Fab structural model at the final stage of CNS refinement, before adding water molecules. An analysis of the final model was performed by using Procheck [26], the status of the final model being summarized in Table 1. The coordinates and structural factors have been deposited in the Protein Databank as entry 1KFA.

Results and discussion

Structural features of Fab 4-B8(8)/E9

The crystal of the GA_4 liganded 4-B8(8)/E9 Fab diffracted up to a 2.7 Å resolution. The crystal structure of 4-B8(8)/E9 Fab was refined at a 2.8 Å resolution to an R-factor (R_{free}) of 23.4% (29.6%). The crystal of GA_4 liganded 4-B8(8)/E9 Fab contained two Fab fragments as an asymmetric unit. These were related with a pseudo twofold axis of NCS, and were almost identical. One of these Fab fragments is analyzed in this report as a representative structure. We also attempted to crystallize the unliganded 4-B8(8)/E9 Fab fragment. Although many crystals were obtained under various conditions, they all showed weak diffraction up to a 3 Å resolution.

The $2F_o$–F_c electron density map was in good agreement with a model incorporating six CDR loops of the heavy and light chains. However, weak electron density was apparent for the C-terminal region of each chain and for the loop region between H114 and H118, and between H132 and H138. These regions are therefore not included in the final model. Weak electron density was also found for L56 and L57; although these residues are included in the final model, they each have an elevated *B*-factor. A Ramachandran plot [27] indicated that the ϕ, ψ torsion angle distribution conformed well with those observed in the refined structures with few exceptions, as has been commonly reported in many antibody structures [28,29] (data not shown).

CDR conformations of 4-B8(8)/E9

The antigen-combining site of antibodies was formed by six loops of the polypeptide chain, involving three loops each from the variable domain of the light chain (CDR-L1, CDR-L2, and CDR-L3), and from the variable domain of the heavy chain (CDR-H1, CDR-H2, and CDR-H3). The relationship between the amino acid sequence of the antigen-combining site and the structure has been well studied [28,30]. The loops of 4-B8(8)/E9 have been determined according to a hypervariable structural definition, while the numbering of the residues follows the widely adopted Kabat numbering scheme [30]. The amino acid sequences of the variable domains of 4-B8(8)/E9 are shown in Fig. 2.

The conformations of the six CDRs of the 4-B8(8)/E9 antibody are shown in Fig. 3. Six CDRs formed loops which were supported by the typical immunoglobulin fold. In the refined structure of the Fab fragment, the $2F_o$–F_c electron density map in the antigen-combining region was well defined. Although CDRs have various sequences and lengths, CDR conformations usually configure canonical structures, except for CDR-H3 [28]. An automated comparison of the observed conformation with those described by the canonical approach (http://www.biochem.ucl.ac.uk/~martin) shows that the hypervariable regions of the 4-B8(8)/E9 antibody are consistent with the following classification, except for CDR-H3 [31].

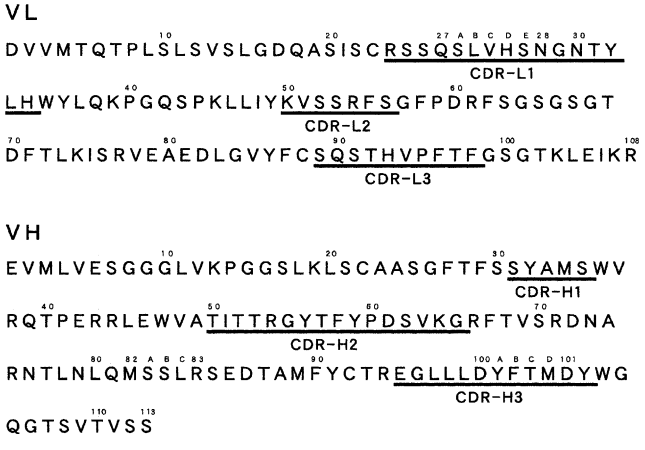

Fig. 2. Amino acid sequences of the variable regions of 4-B8(8)/E9. The sequences are numbered according to the Kabat numbering scheme [31,32]. The three CDRs for each chain are underlined. CDRs were determined according to automated structural definition. Light chain (V_L) L27A-E, heavy chain (V_H) H82A-C, and H100A-D are inserted residues according to the Kabat numbering scheme.

In the light chain, CDR-L1 (L24–L34, 16 residues long) belongs to canonical structure class 4 for the κ light chain (key residues Cys23L and Trp35L). This loop region bridges two β-sheets, and the region is packed across the top of the V_L domain. A three-residue turn (L27E-L29), which is structurally supported by a hydrogen bond between His27DL and Gly29L and is commonly found in all CDR-L1 conformations of canonical structure class 4, constitutes the narrow region of the loop. The second light chain hypervariable region, CDR-L2 (L50–L56, seven residues long), belongs to canonical structure class 1 which has conserved residues (Ile48L and Gly64L). A three-residue hairpin turn (L48–L50) is stabilized by a hydrogen bond between Lys50L and Ser52L. Hypervariable region CDR-L3 (L89–L97, 10 residues long) of 4-B8(8)/E9 belongs to canonical structure class 1 for the κ light chain and forms a hairpin loop which is stabilized by a hydrogen bond between Gln90L and Thr97L. The key residues for canonical structure class 1 of CDR-L3 are Gln90L, Pro95L, and Thr97L.

In the heavy chain, the first hypervariable region CDR-H1 is packed across the top of the V_H domain, bridging the two β-sheets. CDR-H1 of 4-B8(8)/E9 (H31-H35, five residues long) follows the conformation of canonical structure class 1 which is the most commonly observed conformation for an antibody. CDR-H2 of 4-B8(8)/E9 (H50–H65, 16 residues long) belongs to canonical structure class 1, which is the shortest loop in the four CDR-H2 canonical structures. CDR-H2 forms a long hairpin loop with a two-residue turn which is structurally supported by a sheet motif.

As for 4-B8(8)/E9, three CDRs of the light chain and two CDRs of the heavy chain, CDR-H1 and CDR-H2, belong to the canonical structures. On the other hand, CDR-H3 belongs to a non-canonical structure. CDR-H3 of 4-B8(8)/E9 (H95-H102, 12 residues long) forms a unique circular loop which is mainly stabilized by a hydrogen bond between Glu95H and Thr100CH. The hydrogen bond network involving Gly96H, Leu98H, Leu97H, Leu99H, and Asp100H plays an important role in supporting the turn structure of this region.

Antigen-combining site of 4-B8(8)/E9

The F_o–F_c electron density map revealed that the GA_4 molecule was bound in the antigen recognition area (Fig. 4a). The hapten molecules are generally combined in the center of the immunoglobulin fold of an antibody,

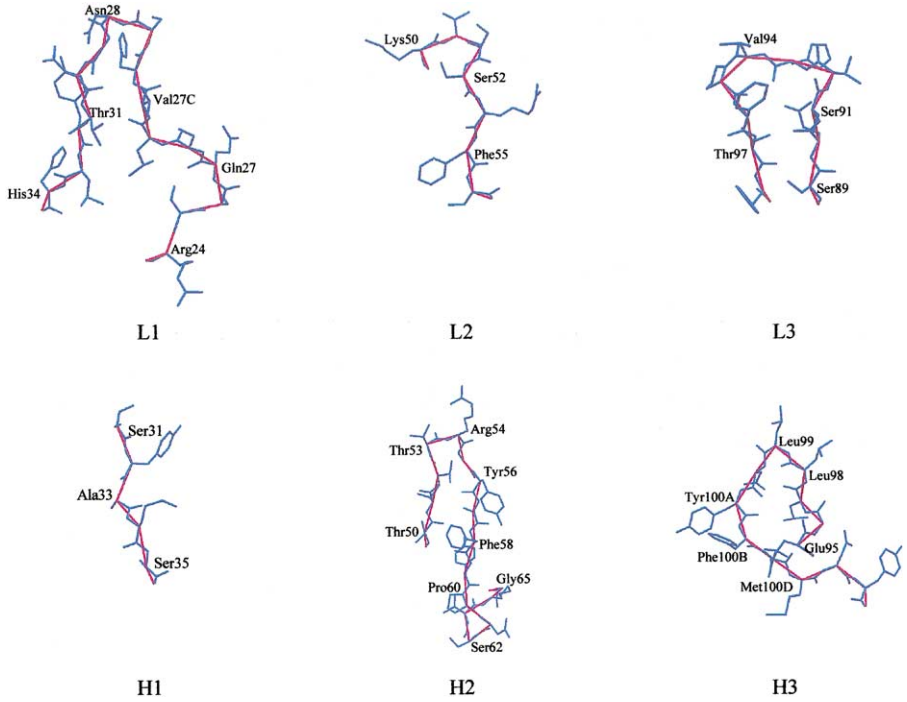

Fig. 3. Conformation of each CDR of 4-B8(8)/E9 Fab. The magenta lines show the Cα trace of the main chain of the CDR loops. Full atom representation of the 4-B8(8)/E9 CDR loops is given by the cyan lines. The figure was generated by Swiss-PdbViewer [33].

but GA_4 existed on the heavy chain side of the 4-B8(8)/E9 Fab antibody (Fig. 4b). The CDR-H3 loop insulates GA_4 from light chain CDRs; thereby, a small cavity in the antigen-combining site was formed by three heavy chain CDRs, and the light chain CDRs did not directly interact with GA_4. CDR-H1 played an important role in the formation of the antigen-combining site, because CDR-H1 had a hydrogen bond with both CDR-H2 and CDR-H3, while CDR-H2 and CDR-H3 did not form any hydrogen bonds. Met34H of CDR-H1, and Thr50H and Ile51H of CDR-H2 were involved in forming the hydrogen bonds with those two CDRs. The hydrogen bond between CDR-H1 and CDR-H3 was formed by Ser35H of the former, and by Tyr100AH and Phe100BH of the latter CDR. On the other hand, the interactions between CDR-H2 and CDR-H3 were only due to van der Waals contact. Namely, the two aromatic residues Tyr56H and Phe58H of CDR-H2 and Tyr100AH and Phe100BH of CDR-H3 interacted hydrophobically with each other and thus provided a hydrophobic region for the antigen-combining site.

Antibody–GA_4 interaction

The interaction between GA_4 and 4-B8(8)/E9 Fab is summarized in Fig. 4c. It has been shown from the results of a cross-reactivity analysis with various GA analogs that the 3β-hydroxyl and 6β-carboxyl groups were important for the GA_4 recognition by 4-B8(8)/E9 [2]. In particular, 4-B8(8)/E9 showed no specificity toward the lactone ring of the GA molecules, such that both γ-lactone and δ-lactone were accepted by the antibody with high affinity (Fig. 1). The crystal structure of 4-B8(8)/E9 Fab complexed with GA_4 had no hydrogen bond formed between the antibody and γ-lactone ring of GA_4. It was revealed that the 3β-hydroxyl and 6β-carboxyl groups of the GA_4 molecule were the main targets in ligand recognition. On the other hand, the very hydrophobic regions on the C/D rings of GA_4 resulted in van der Waals interaction with the antibody by its β-face on the C/D rings of the molecule. Tyr56H and Phe58H of CDR-H2 and Tyr100AH and Phe100BH of CDR-H3 formed the base of the cavity of the antigen-combining site with their side chains and provided a hydrophobic region to accept the C/D rings of GA_4. Tyr100AH and Phe100BH made van der Waals contact with GA_4. Phe100BH played a particularly critical role in antigen binding by forming a stacking interaction with the β-side on the C ring of the GA_4 molecule. Thr52H made van der Waals contact with the 6β-carboxyl group of GA_4.

Leu98H and Leu99H were present in the apical region of the CDR-H3 loop, and were stacked with the GA_4 molecule from the top of the antigen-binding site. This region had a relatively low *B*-factor, probably because of binding of the antigen and crystal packing interaction. The antigen-combining site of 4-B8(8)/E9 may be open when the antigen is absent. We infer that this is a reason why the liganded crystals diffracted to a higher resolution than that of the unliganded crystals.

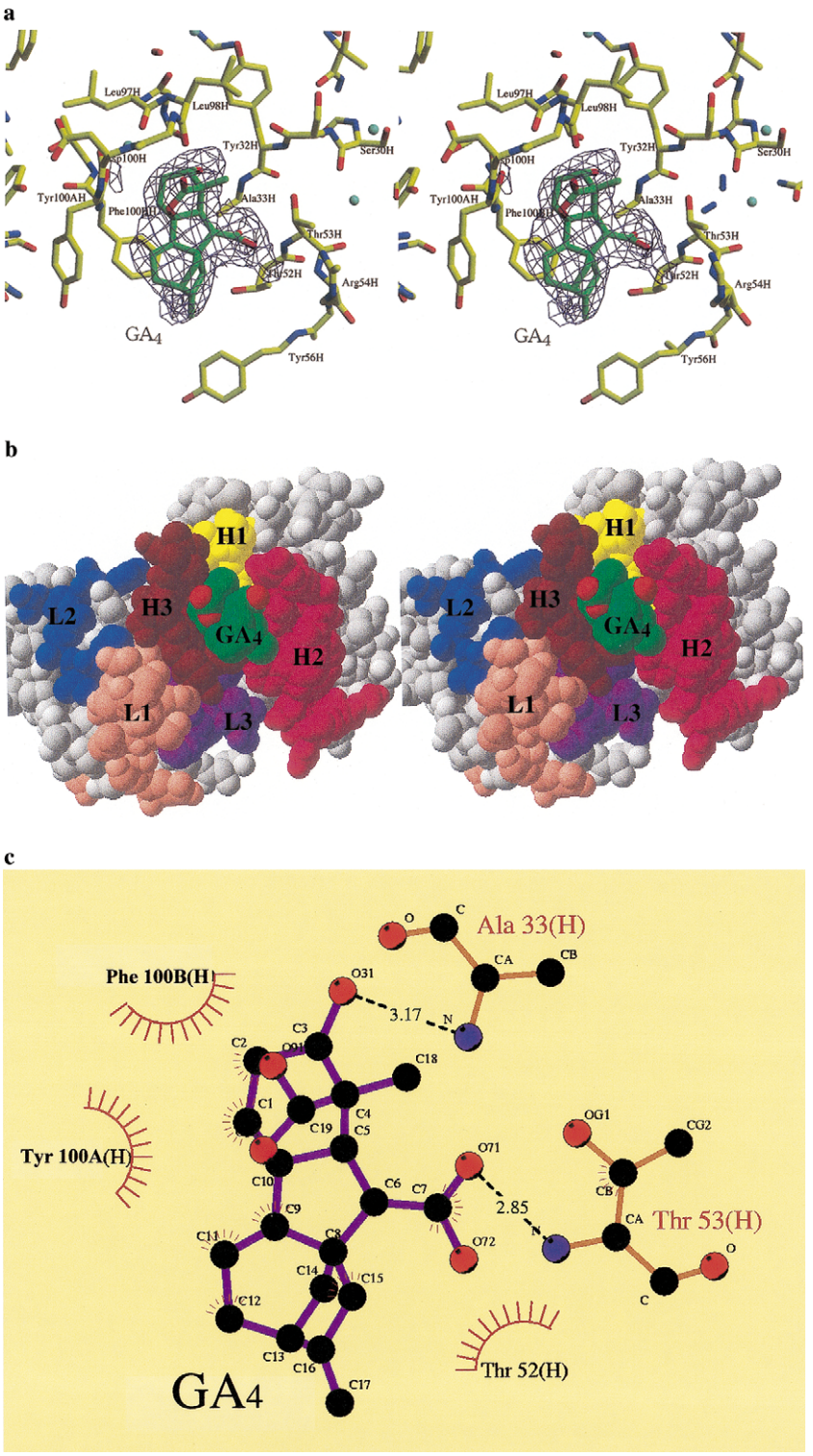

Fig. 4. Ligand-combining models of 4-B8(8)/E9 Fab. Some residues are labeled by their sequence number. (a) Stereo drawing of the plan view focused on the antigen-combining region. The carbon skeleton of GA_4 is green, and protein carbon atoms are yellow. The F_o–F_c electron density map is superimposed. The figure was prepared by using XtalView [34] and rendered by Raster3D [35]. (b) Space-filling representation of the variable domain of the liganded Fab viewed from the antigen-combining site in stereo. CDR loops are drawn in light pink (L1), blue (L2), purple (L3), yellow (H1), magenta (H2), and red (H3). Carbon and oxygen atoms of GA_4 are drawn in green and red, respectively. Frame regions for each chains are drawn in grey. The figure was generated by using Swiss-PdbViewer [33]. (c) Schematic drawing of the interaction between GA_4 and 4-B8(8)/E9 Fab. The figure was generated by LIGPLOT [36].

This is the first report on the crystallographic structure of the anti-plant hormone antibody. Further experiments are required to obtain the required useful information to construct an scFv that is capable of specific and tight conjugation against GAs. The crystallographic analysis of the conjugates of GAs and their metabolic enzymes, which has not yet been reported, will provide further information about the manner of recognition of the functional groups that characterize the nature of each GA, and help us to build an effective scFv.

Acknowledgments

Bio-oriented Technology Research Advancement Institution (BRAIN) of Japan financially supported I.Y. in this research. We thank the staff of the Photon Factory for their assistance with the data collection.

References

[1] P.J. Davies, Plant Hormones: Physiology, Biochemistry and Molecular Biology, second ed., Kluwer Academic Publishers, Netherlands, 1995.

[2] M. Nakajima, I. Yamaguchi, A. Nagatani, S. Kizawa, N. Murofushi, M. Furuya, N. Takahashi, Monoclonal antibodies specific for non-derivatized gibberellins I. Preparation of monoclonal antibodies against GA_4 and their use in immunoaffinity column chromatogaphy, Plant Cell Physiol. 32 (1991) 515–521.

[3] Y. Suzuki, N. Shimada, R. Niwa, M. Yokoi, M. Nakajima, N. Murofushi, I. Yamaguchi, Preparation and application of anti-idiotypic antibody against anti-gibberellin A_4 antibody, Biosci. Biotechnol. Biochem. 63 (1999) 648–654.

[4] N. Shimada, Y. Suzuki, M. Nakajima, U. Conrad, N. Murofushi, I. Yamaguchi, Expression of a functional single-chain antibody against $GA_{24/19}$ in transgenic tobacco, Biosci. Biotechnol. Biochem. 63 (1999) 779–783.

[5] G.D. Jaeger, C.D. Wilde, D. Eeckout, E. Fiers, A. Depicker, The plantibody approach: expression of antibody genes in plants to modulate plant metabolism or to obtain pathogen resistance, Plant Mol. Biol. 43 (2000) 419–428.

[6] U. Conrad, U. Fiedler, Compartment-specific accumulation of recombinant immunoglobulins in plant cells: an essential tool for antibody production and immunomodulation of physiological functions and pathogen activity, Plant Mol. Biol. 15 (1998) 281–293.

[7] Y. Li, H. Li, J. Sandra, S.J. Smith-Gill, R.A. Mariuzza, Three-dimensional structures of the free and antigen-bound Fab from monoclonal antilysozyme antibody HyHEL-63, Biochemistry 39 (2000) 6296–6309.

[8] P.M. Colman, W.G. Laver, J.N. Verghese, A.T. Baker, P.A. Tulloch, G.M. Air, R.G. Webstar, Three-dimensional structure of a complex of antibody with influenza virus neuraminidase, Nature 326 (1987) 358–363.

[9] W.R. Tulip, J.N. Verghese, W.G. Laver, R.G. Webstar, P.M. Colman, Refined crystal structure of the influenza virus N9 neuraminidase-NC41 Fab complex, J. Mol. Biol. 227 (1992) 122–148.

[10] R.L. Malby, W.R. Tulip, V.R. Harley, J.L. McKimm-Breschkin, W.G. Laver, R.G. Webstar, P.M. Colman, The structure of a complex between the NC10 antibody and influenza virus neuraminidase and comparison with the overlapping binding site of the NC41 antibody, Structure 2 (1994) 733–746.

[11] S.E. Mylvaganam, Y. Paterson, E.D. Getzoff, Structural basis for the binding of an anti-cytochrome *c* antibody to its antigen: crystal structures of FabE8-cytochrome *c* complex to 1.8 Å resolution and FabE8 to 2.26 Å resolution, J. Mol. Biol. 281 (1998) 301–322.

[12] M. Huang, R. Syd, E.A. Stura, M.J. Stone, R.S. Stefanko, W. Ruf, T.S. Edgington, I.A. Wilson, The mechanism of an inhibitory antibody on TF-initiated blood coagulation revealed by the crystal structures of human tissue factor, Fab 5G9 and TF.G9 complex, J. Mol. Biol. 275 (1998) 873–894.

[13] L. Prasad, S. Sharma, M. Vandonselaar, J.W. Quail, J.S. Lee, B. Waygood, K.S. Wilson, Z. Dauter, T.J. Delbaere, Evaluation of mutagenesis for epitope mapping. Structure of an antibody–protein antigen complex, J. Biol. Chem. 268 (1993) 10705–10708.

[14] P. Bossart-Whitaker, C.Y. Chang, J. Novotny, D.C. Benjamin, S. Sheriff, The crystal structure of the antibody N10-staphylococcal nuclease complex at 2.9 Å resolution, J. Mol. Biol. 253 (1995) 559–575.

[15] T. Bizebard, B. Gigant, P. Rigolet, B. Rasmussen, O. Diat, P. Bosecke, S.A. Wharton, J.J. Skehel, M. Knossow, Structure of influenza virus haemagglutinin complexed with a neutralizing antibody, Nature 376 (1995) 92–94.

[16] Y.A. Muller, Y. Chen, H.W. Christinger, B. Li, B.C. Cunninghum, H.B. Lowman, A.M. de Vos, VEGF and the Fab fragment of a humanized neutralizing antibody: crystal structure of the complex at 2.4 Å resolution and mutational analysis of the interface, Structure 6 (1998) 1153–1167.

[17] D.T. Nair, K. Singh, N. Sahu, K.V. Rao, D.M. Salunke, Crystal structure of an antibody bound to an immunodominant peptide epitope: novel features in peptide-antibody recognition, J. Immunol. 165 (2000) 6949–6955.

[18] J.P. Derrick, R. Urwin, J. Suker, I.M. Feavers, M.C. Maiden, Structural and evolutionary influence from molecular variation in *Neisseria porins*, Infect. Immun. 67 (1999) 2406–2413.

[19] P. Dokurno, P.A. Bates, H.A. Band, L.M.D. Stewart, J.M. Lally, J.M. Burchell, J. Taylor-Papadimitriou, D. Snary, M.J.E. Sternberg, P.S. Freemont, Crystal structure at 1.95 Å resolution of the breast tumor-specific antibody SM3 complexed with its peptide epitope reveals novel hypervariable loop recognition, J. Mol. Biol. 284 (1998) 713–728.

[20] R. Kodandapani, L. Veerapandian, C.Z. Ni, C.K. Chiou, R.M. Whittal, T.J. Kunicki, K.R. Ely, Conformational change in an anti-integrin antibody: structure of OPG2 Fab bound to a beta 3 peptide, Biochem. Biophys. Res. Commun. 251 (1998) 61–66.

[21] A.G.W. Leslie, Crystallographic Computing, Oxford University Press, Oxford, London, 1990.

[22] A.T. Brunger, P.D. Adams, G.M. Clore, W.L. Delano, P. Gros, R.W. Grosse-Kunstleve, J.S. Jiang, J. Kuszewski, M. Nilges, N.S. Pannu, R.J. Read, L.M. Rice, T. Simonson, G.L. Warren, Crystallography and NMR system: a new software suite for macromolecular structure dtermination, Acta Cryst. D 54 (1998) 905–921.

[23] D. Altschuh, O. Vix, B. Rees, J.C. Thierry, A conformation of cyclosporin A in an aqueous environment revealed by the X-ray structure of a cyclosporin–Fab complex, Science 256 (1992) 92–94.

[24] O. Almog, I. Benhar, G. Vasmatzis, M. Tordova, B. Lee, I. Pastan, G.L. Gilliland, Crystal structure of the disulfide-stabilized Fv fragment of anticancer antibody B1: conformational influence of an engineered disulfide bond, Proteins 31 (1998) 128–138.

[25] Jones, T.A., Kjeldgaard, M., 1995. O the Manual, Version 5.10, Uppsala, Sweden.

[26] R.A. Lascowski, M.W. MacArthur, D.S. Moss, J.M. Thornton, PROCHECK: a program to check the stereochemical quality of protein structures, J. Appl. Cryst. 26 (1993) 283–291.

[27] G.N. Ramachandran, V. Sasisekharan, Conformations of polypeptides and proteins, Adv. Protein Chem. 23 (1968) 283–437.
[28] B. Al-Lazikani, A.M. Lesk, C. Chothia, Standard comformations for he canonical structures of immunoglobulins, J. Mol. Biol. 273 (1997) 927–948.
[29] E.J. Milner-White, B.M. Ross, R. Ismail, K. Belhadj-Mostefa, R. Poet, One type of gamma-turn, rather than the other gives rise to chain-reversal in proteins, J. Mol. Biol. 204 (1988) 777–782.
[30] C. Chothia, J. Novotny, R.E. Bruccoleri, M. Karplus, Domain association in immunoglobulin molecules: the packing of variable domains, J. Mol. Biol. 186 (1985) 651–663.
[31] A.C.R. Martin, Accessing the Kabat antibody sequence database by computer, Proteins 25 (1997) 130–133.
[32] Kabat, E.A., Wu, T.T., Bilofski, H., 1979. Sequences of immunoglobulin chains. National Institute of Health NIH Publication, 80-2008.
[33] N. Guex, M.C. Peitsch, SWISS-MODEL and Swiss-PdbViewer: an environment for comparative protein modeling, Electrophoresis 18 (1997) 2714–2723.
[34] D.E. McRee, XtalView/Xfit—a versatile program for manipulating atomic coordinates and electron density, J. Struct. Biol. 125 (1999) 156–165.
[35] E.A. Merritt, D.J. Bacon, Raster3D: photorealistic molecular graphics, Methods Enzymol. 277 (1997) 505–524.
[36] A.C. Wallace, R.A. Laskowski, J.M. Thornton, LIGPLOT: a program to generate schematic diagrams of protein–ligand interactions, Protein Eng. 8 (1995) 127–134.